Multiple Phase Silicon in Submicrometer Chips Removed by Diamond Turning

R. G. Jasinevicius
A. J. V. Porto
and J. G. Duduch
Departamento de Engenharia Mecânica
EESC-Universidade de São Paulo
13560-590 São Carlos, SP. Brazil
renatogj@sc.usp.br, ajvporto@sc.usp.br
jgduduch@sc.usp.br

P. S. Pizani and F. Lanciotti Jr.
Departamento de Física
Universidade Federal de São Carlos
13565-905 São Carlos, SP. Brazil
pizani@df.ufscar.br, lanciott@df.ufscar.br

F. J. dos Santos
Departamento de Física- CCET
Universidade Federal de Mato Grosso do Sul
790709-900 Campo Grande, MS. Brazil
francisco_js@yahoo.com

Continuous chips removed by single point diamond turning of single crystal silicon have been investigated by means of Scanning Electron Microscopy/Transmission Electron Microscopy and micro-Raman Spectroscopy. Three different chip structures were probed with the use of electron diffraction pattern: (i) totally amorphous lamellar structure, (ii) amorphous structure with remnant crystalline material and, (iii) partially amorphous together with amorphous with remnant crystalline material. Furthermore, micro-Raman spectroscopy from the chips left in the cutting tool rake face showed different silicon phases. We have found, from a detailed analysis of the debris, five different structural phases of silicon in the same debris. It is proposed that material removal mechanisms may change along the cutting edge from shearing (yielding lamellar structures) to extrusion. Shearing results from structural changes related to phase transformation induced by pressure and shear deformation. Extrusion, yielding crystalline structures in the chips, may be attributed to a pressure drop (due to an increase in the contact area) from the tool tip towards the region of the cutting edge where brittle-to-ductile transition occurs. From this region upwards, pressure(stress) would be insufficient to trigger phase transformation and therefore amorphous phase would not form integrally along the chip width.
Keywords*: Silicon, diamond turning, material removal mechanism, phase transformation*

Introduction

Monocrystalline semiconductors are normally considered to be fragile and to exhibit brittle response under conventional machining conditions. In ultraprecision diamond turning of brittle materials, it is well-established that under particular critical conditions of depth and/or thickness of cut, it is possible to achieve ductile mode material removal so as to generate a crack free surface (Blake and Scattergood 1990, Marshal et al., 1983, Puttick et al., 1989). The great interest in achieving ductile machining of semiconductors is concerned with the possibility of obtaining mirror-like surface finish and low subsurface damage.

Recently, new concepts have been applied to explain the anomalous plasticity presented by semiconductor crystals during mechanical material removal processes such as single-point diamond turning and diamond grinding at room temperature. One such concept is related to amorphous structures found in machined surfaces by means of different techniques such as Transmission Electron Microscopy (Puttick et al., 1994) and Raman Spectroscopy (Pizani et al., 1999). This amorphization in machined surfaces has been correlated to plastic behaviour since monocrystalline materials exhibit limited dislocation mobility and, consequently, brittle behaviour below 650 °C (Susuki and Ohmura, 1996). This phase transformation takes place because a very high hydrostatic pressure with a high shear component develops at the point of contact between the tool edge and the machined material. The ductile mode machining of silicon may therefore be related to a pressure induced structural transformation. The description of the mechanism involved in ductile chip formation is still open to question and motivated this study.

Paper accepted July, 2005. Technical Editor: Anselmo Eduardo Diniz.

This study aims to present an original contribution on the mechanism of chip formation at submicrometre depths of cut. The investigation will contribute to a better understanding of the mechanics of ductile material removal of silicon. This is a start towards elucidating the effect of phase transformation upon material removal mechanism.

Facing cuts were conducted on a diamond turning machine tool under suitable cutting conditions that generated ductile mode material removal of single crystal silicon. Based on the results of TEM analyses of the chips, the material removal mechanism was determined and a model of chip formation under decompression proposed. Micro-Raman spectroscopy detailed analysis of the chips left on the tool rake face was carried out. Five different structural phases of silicon were found in the chip. Based upon these findings, a new concept to interpret the ductile material removal mechanism during the machining process was proposed. The implications of the results on the understanding of the ductile to brittle transition are also discussed.

Review of the Literature

Although the machining of materials seems a simple mechanical process of matter separation, it involves complex phenomena of high-pressure physics, phase transitions, elastic properties of matter and chemical affinity between the cutting tool edge and machined materials. Furthermore, the material removal mechanism involved in the machining of semiconductor crystals with single point diamond tools may be considered one of the richest processes to generate structural phase transformations. The plastic behaviour of silicon during diamond turning has been attributed to a pressure induced structural transformation from diamond cubic structure to a metallic characteristic (Morris et al., 1995). This proposition was based on earlier studies on high hydrostatic pressure (Jamieson, 1963; Minomura and Drickamer, 1962), microindentation (Gridneva et al., 1972; Clarke et al., 1988) and Scratching (Minowa and Sumino,

1992) which had demonstrated that diamond-cubic silicon transforms to the denser metallic β-tin structure at room temperature. In silicon, the critical pressure observed to cause the transformation to a β-tin metallic phase is in the range of 11.3-12.5 GPa and the pressure to cause transformation into the metastable amorphous semiconductor phase, upon unloading, is about 7.5-9.0 GPa (Hu et al., 1986). The presence of shear strain components lowers the transition pressure value (Gilman, 1992; Gupta and Ruoff, 1980; Minowa and Sumino, 1992). According to Gilman (1993), a combination of isotropic compressive and shear strains (uniaxial compression) induces the transition to the metallic state under much lower stresses than those required for isotropic compression. This may produce a favorable effect on machining processes. Gupta and Ruoff (1980) reported a difference of 40 % in the pressure to transform silicon to a metallic phase when loaded in the [111] direction (~8.5 GPa) and in the [100] direction (12GPa).

Experimental works presenting indirect evidences of the effect of high hydrostatic pressure (inducing phase transformation) on the ductile material removal in the machining of semiconductor crystals have been reported (Morris et al., 1995; Puttick et al., 1994; Shibata et al., 1994). TEM results not only provided information on the surface and subsurface integrity of diamond turned semiconductors crystals, but also gave support to propose the material removal mechanisms involved. Researchers did not agree on the estimated thickness of the amorphous layer. While Puttick et al. (1994) found 100-400 nm in ground Si (111), Shibata et al. (1994) found 100 nm and 500 nm for 2 and 3 micrometre depths of cut, respectively, for single point diamond turned Si (100). In addition, it was found that the layer of the diamond turned surface presented remnant crystalline phase embedded in an amorphous phase for both germanium (Morris et al., 1995) and silicon (Jasinevicius et al. 2000a). Therefore, it has to be taken into consideration that the amorphous/crystalline phase, probed in a diffraction scale, is likely to be considered as a polycrystal formed by nanocrystals (Suzuki and Ohmura, 1996). This result corroborated very well with Raman spectroscopy results lately reported by Pizani et al. (1999) in which the shortening of the phonon correlation length was indicative that at the vicinity of the surface the layer was composed of silicon crystallites immersed in a silicon amorphous medium. Furthermore, the works reported to date do not agree on what the primary mechanism of material removal is. While Shibata and collaborators (1994) and Jasinevicius et al. (2000 a) found only amorphous structure in silicon chips, Morris and collaborators (1995) found crystalline and amorphous phase in germanium chips. These conclusions brought about a question: how can the surface be composed of silicon crystallites immersed in a silicon amorphous medium and the chips be totally amorphous? It is essential to arrive at an agreement on this matter for the comprehension and domain of the mechanisms responsible for introducing deleterious damage into the surface and subsurface. Puttick et al. (1994) proposed a material removal mechanism in silicon based upon extrusion of the plastically deformed material ahead of the tool. This result was confirmed by Komanduri et al. (2001) who based their analyses on Molecular Dynamics (MD). Komanduri et al. (2001) proposed that there existed four mechanisms involved in material removal namely: i) compression of the work material ahead of the tool in the primary deformation region; ii) formation of the chip by a mechanism similar to extrusion process; iii) subsurface deformation of the material underneath the tool in the machined surface; and iv) lateral flow. It is worth mentioning that the chip formation process is characterised by (Shaw, 1984): i) extremely large strains (200-300%); ii) extremely large strain rates (10^4 - 10^6 second^{-1}); iii) rubbing of a freshly formed surface which is clean and chemically active against the tool rake face; iv) rubbing between the newly created surface and some portion worn tool clearance face and elastically pressing against the surface. It should be mentioned that the studies by Komandury and collaborators presented a strictly nanometric level analysis. Despite the results offered by Puttick et al (1994) and Komanduri et al (2001), other studies using TEM did not show the same evidences. Morris et al (1995) observed two types of ductile chips removed from single crystal germanium, namely Type A which is amorphous, as shown by diffraction and diffuse dark field imaging, and Type B whose morphology differs from type A in two respects: There are a large number of holes and small dark blotches and a (110) polycrystalline texture displayed by electron diffraction and formed by microfracture (pitting) in areas of the wafer having the highest resolved tensile stresses on cleavage planes. According to the authors, subsequent passes of the tool would lift these crystallites to a plasticized zone, apparently maintaining their initial orientation with respect to the surface, as shown in Figure 1.

However, to accept this consideration, the cut would have to be restricted to a submicrometre range depth of cut, which was not the case (according to the authors the depth of cut was 10μm). Figure 2 a) gives a schematic diagram illustrating the machining geometry with round nose tool. The crystallites formed at the surface vicinity have to be removed by the uppermost position of the tool on the uncut shoulder, as shown schematically in Figure 2 b and the corresponding portion of the chip is too thick to have been examined with TEM.

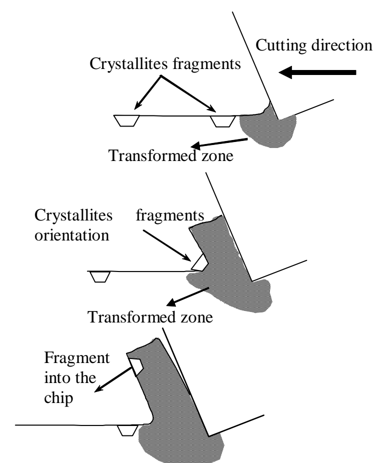

Figure 1. Schematic illustration of chip and microcrystallite orientation during cutting (after Morris et alli 1995).

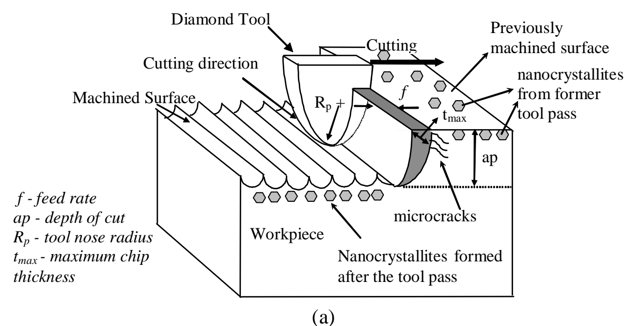

Figure 2. a) Schematic diagram of the cutting geometry for single point diamond turning with round nose tools and typical chip formed during totally ductile chip removal; b) In the diagram *f* is the feed rate (μm/rev), tc is the brittle-to-ductile transtion point, yc is the fracture damage depth. The Ductile chip formation occurs within the Z_{ef} region; b) typical chip removed when the process takes place in the ductile mode. The arrow shows a thin part of the chip detaching from the main body of the chip (reproduced partially after Blake and Scattergood,1990).

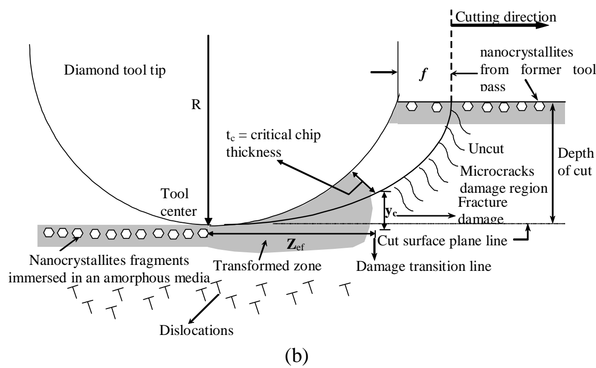

(b)

Figure 2. (Continued).

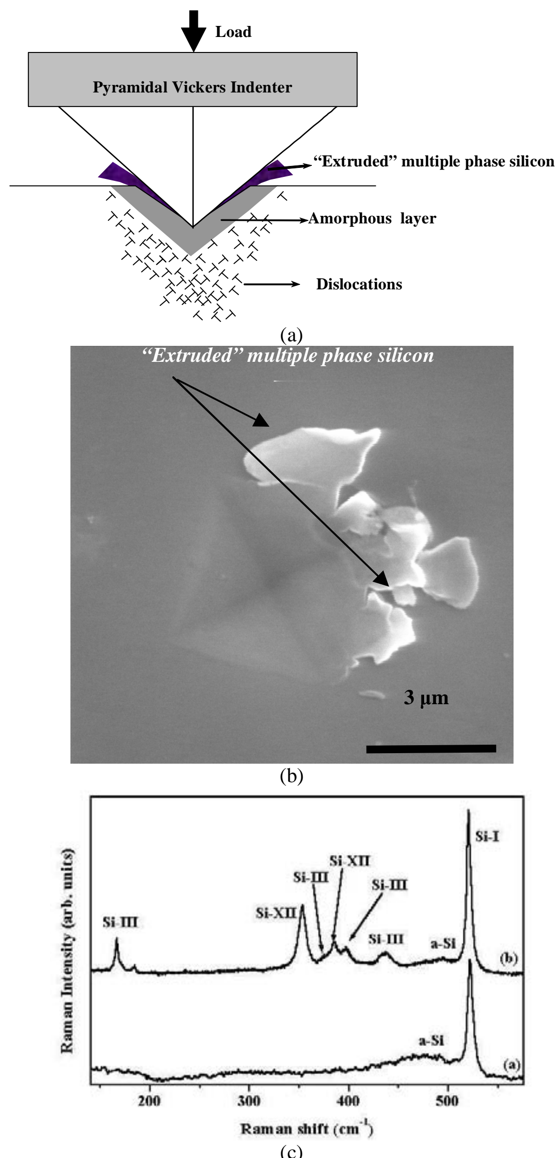

Figure 3. a) schematic drawing showing the mechanism akin to extrusion-like process in microindentation; b) SEM photomicrograph of a Vickers indentation impression (load: 150 mN) load/unload cycle of 10 times. There is an amount of plastically extruded material around the impression;. c) Raman spectra of Vickers indentations in Si made by load/unload cycles with 150 mN showing two distinct situations: (a) the detection of amorphous Si for 5 steps and (b) and high pressure phases for the indent made by 10 steps.

On the other hand, Morris et al. (1995) agree that the presence of crystalline fragments could be correlated to those detected around plastic extrusions observed in low load indentations in silicon (Callahan and Morris, 1992). According to Kailer et al. (1997) metallic Si-II has lower yield stress than original diamond structure Si and is easily pressed out at the indentation boundary. Moreover, in indentation the innermost part of the indentation mark is amorphous (Clarke et al. 1988; Suzuki and Ohmura 1996; Wu and Xu in 1998) as much as the Type A chips. It is worth noting that such correlation with low load indentation would imply that such extruded portions of material are likely originated from the upper portion of the indenter, as shown in Figure 3a. However, the "plastic extrusion" of material at the borders, generating multiple crystalline phase (similar to Type B chip) is only formed after repetitive cycles. A typical Vickers microhardness impression for 150 mN obtained with cyclic microindentation load is shown in Figure 3 b). Observe that there is plastically extruded material around the impression. This microindentation impression was the final deformation microstructure of 10 steps (i.e., consecutive load/unloading cycles) (Jasinevicius and Pizani, 2004). The Raman spectra presented in Figure 3 c) were obtained under two different situations: (a) after 5 steps and; (b) after 10 steps.The microstructure formed in the central region of the impression formed with 5 steps is amorphous with Raman spectrum showing characteristic broad band at about 470 cm^{-1}. However, the spectrum from the "extruded" silicon around the impression formed with 10 steps, shows the formation of a number of bands characterized as arising from Si-III (bc8, body-centred cubic structure) with the bands at 166, 382, and 433 cm^{-1} and Si-XII (r8, the rhombohedral distortion of bc8) with the bands at 350 and 394 cm^{-1}. The pattern of increasing steps giving rise to polycrystalline deformation microstructures has been investigated for spherical indentation by Raman spectroscopy (Bradby et al. 2001; Zarudi et al. 2003b) as well as with TEM technique (Zarudi and Zhang, 1999; Zarudi et al.2003a; 2003c; 2004). According to the reported works the amorphous silicon phase can be decomposed to crystalline R8/BC8 phases during the consecutive repeated indentations. In addition, the works reported on cyclic indentations demonstrated that upon single unloading Si-II (β-Sn) is transformed into the amorphous state, but after consecutive repeated steps the amorphous phase formed after the first indentation can be decomposed to crystalline Si-III/Si-XII phases during consecutive repeated indentations. This multiple crystalline phase found in the extruded silicon cyclic indentations could be related to Type B chips. However, despite the observation of phase transition in microindentation, it is worth mentioning that this is a quasi-static process which is far different from machining.

Gogotsi et al. (2001) probing wear debris generated by scratching silicon with indenters of different geometries also detected policrystalinity. Besides amorphous silicon, they found Si-III, SiXII and Si-IV. In both indentation and scratching, amorphous silicon was probed by Gogotsi and collaborators at smaller depths of cut while Si-III, Si-XII and Si-IV formed at larger depths of cut. According to them, since the scratching experiments were conducted at constant speed, at a small depth of cut, the residual stresses were relatively small. This leads to a faster stress decrease than at a large depth, when significant residual stresses and the constraint of surrounding material results in a slow reverse transformation (*idem*). Therefore, amorphous silicon was formed at a small depth of cut, while Si-III, Si-XII and Si-IV were formed at a larger depth of cut (*idem*). At very small depths, the contact pressure is larger and only amorphous phase was evidenced while with the increase in depth the width of contact also increases, decreasing the pressure of contact, favouring the formation of Si-III, Si-IV and Si-XII (idem). Finally, the metastable phases (Si-III and Si-XII) along with amorphous silicon in the scratches supports the

fact of pressure induced phase trasnformation during scratching. This is an important finding since during scratching there is a dynamic component which is similar to machining process.

It can be seen from this brief review that, despite all the efforts towards the comprehension of the mechanisms involved in material removal and chip formation during micromachining of semiconductors crystals, there still remain some questions: Are the different phases found in the chips really formed from areas of the wafer having the highest resolved tensile stresses on cleavage planes or may they be resultant from the variation of contact pressure between the tool rake face and material along the width of cut? Is it possible to find different phases within the same chip? Is fracture in the thicker portion of the uncut shoulder in the cutting model presented by Blake (1988) a result of insufficient contact pressure or is it just a case to be analysed by fracture mechanics? The analyses of chips removed at submicrometer range depth of cut can help to elucidate the phenomena occurring at the same dimension that the surface is being generated.

Experiments

The specimens were in the form of squares (10 x 10 mm) cut from silicon wafers (100) 1-10 Ω.cm type p (B – 10^{15}-10^{16} atoms/cm^3) of 55 mm diameter and 500 μm thick with surface orientation .

The surface of a crystalline silicon sample with (100) orientation was face-turned with a round nose diamond tool with nose radius of 0.658 millimetres, – 25 degree rake angle and a 12 degree clearance angle from Contour Fine Tooling® (UK). A Rank-Pneumo™ (Keene, NH, US) ASG 2500 diamond turning machine was used in the tests. The spindle rotation speed was kept constant at 1000 rev min^{-1}. The cutting fluid used was a synthetic water soluble oil with the purpose of cooling. This fluid was continuously mist sprayed onto the workpiece during machining. The feedrate used was 2.5 μm/rev and the nominal depth of cut was kept constant at 5 μm. This provides the removal of chips with electron transparency. The crossfeed direction was from the border to the centre of the specimen. These conditions provided ductile mode machining and very thin chips. The surface roughness of the specimens was evaluated by means of an Atomic Force Microscope (Digital Nanoscope IIIa).

A scanning electron microscope (SEM) (LEO, Model 440) at 20 kV was used for the observations of the chips after machining. An Energy Dispersive Spectroscopy (EDS) (OXFORD, detector 7060 Si-Li with system resolution of 113 eV) attached to the SEM was used in this study. The chips observed were those left on the machined surface after the cutting tests. With the combination of EDS and SEM, the elemental compositions of the chip and the surface could be obtained.

A Transmission Electron Microscope (Philips CM200), operated at 200 kV was used to observe the chips and surface. The silicon chips collected from the tool rake face were suspended in isopropyl alcohol, and the mixture was then deposited onto a copper TEM grid (Formvar support or lacey carbon film). The “sandwiched” procedure was used to prepare the cross-sectional sample. The sample for the cross section observation was cut into 2 mm x 2 mm squares, lapped and polished with 5 μm and 1 μm SiC abrasive from the unmachined surface to a thickness of < 50 μm. The sample was then affixed to a copper-slotted TEM grid using epoxy and then dimpled via argon ion milling to provide an electron-transparent central area. In order to allow a clear observation of the amorphized region, low angle ion-beam thinning of short duration was carried out during intervals of TEM observations.

The micro-Raman spectroscopy study was performed with the conventional T64000 Jobin Yvon spectrometer. The 488 nm line of an argon ion laser, focused by an optical microscope on a region of about 1 μm^2 of the tool surface was used to excite the Raman spectrum. Under optical microscope it can be possible to distinguish clearly regions where there are silicon debris, some of them with an aspect of fused material and regions of the tool free of debris.

Results

AFM of a surface produced by diamond turning in a fully ductile mode is shown in Figure 4. No signs of surface damage can be observed. The cross-feed of the cutting tool is 2.5 μm rev^{-1}. The cut grooves are regularly spaced and run parallel to the cutting direction which confirms the absence of chatter vibration. The surface roughness is 1.47 nm Ra.

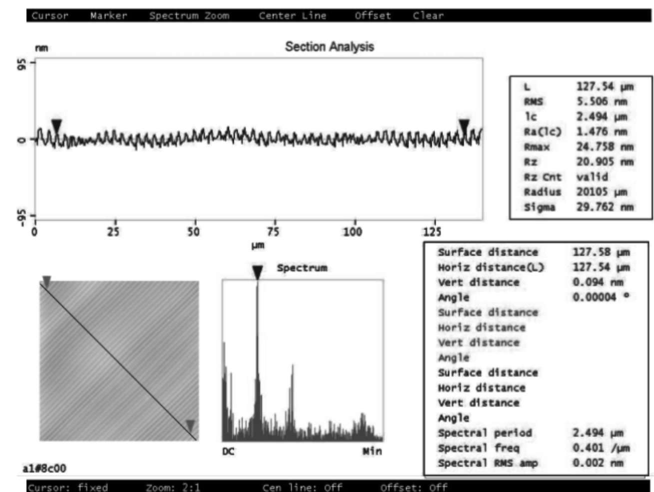

Figure 4. Section analyses made by atomic force microscope of the single-point diamond turned specimen surface finish. The surface finish is smooth and damage-free.

Figures 5 a and 5 b show the Raman spectra of machined silicon samples excited with 457.9 nm and 487.9 nm, respectively. Besides the characteristic Raman peak at 521 cm^{-1} from crystalline silicon, the spectra are characterized by the presence of a broad and less intense band at about 475 cm^{-1}. This band can be ascribed to the optical band of the amorphous silicon (a-Si) and is indicative that the machining took place in the ductile mode. It is interesting to note that, by changing the exciting wavelength from 457.9 nm to 487.9 nm, the intensity of the crystalline peak is increased by a factor of approximately 6, followed by a reduction of the linewidth from about 6 cm^{-1} to 4 cm^{-1}, for the same intensity of the amorphous band in both spectra. According to previous results [Pizani et al. 1999 and Jasinevicius et al. 2000] it was proposed that ductile machining leads to the generation of a crystalline phase immersed in an amorphous medium at the surface. The comparison of the present results with those from Pizani et al. (1999) indicates that the 457.9 nm line is probing the amorphous layer whereas the 487.9 nm line can reach the crystalline layer. The penetration depths of the 457.9 nm and 487.9 nm lines in the crystalline silicon are about 140 nm and 270 nm, respectively, and reduce to about tens of nanometers in the case of a-Si. Considering both spectra presented, it is possible to assert that there is the presence of crystalline phase within the amorphous medium.

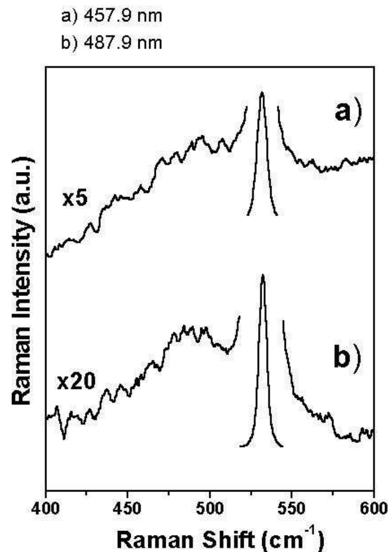

Figure 5. Raman spectra of the machined surface. (a) Raman spectrum of machined sample excited with 457.9 nm; (b) Raman spectrum of the machined silicon sample excited with 487.9 nm.

Figure 6 shows a cross-sectional morphology of the diamond turned surface. The glue layer closely attached to it in Figure 6 shows that the amorphized layer was not damaged during ion-beam machining. A region having a uniform dark grey contrast can be seen in the outermost surface where cutting took place. The thickness of this amorphous layer was estimated to be around 20-30 nm. Dislocation arrays and subsurface microcracks are found beneath this amorphous layer. Dislocation penetration depths are in the range of 100-200 nm (Figure 6). The dislocations observed are strong evidence of the occurrence of plastic deformation generated in front of the cutting tool in the primary deformation zone and third deformation zone from the contact between the flank face and the new surface formed. The diffraction spots, shown in the detail of Figure 6 are from the portion of material within the amorphous layer and subsurface.

After machining, the diamond bit is full of small debris whose dimensions are very small compared to the machining dimensions. Figure 7 displays a Raman spectrum of silicon debris left on the tool surface. In addition to the well known peak at 521 cm^{-1} due to cubic diamond structure of silicon single crystal (Si-I), there are several additional peaks at:1) 519 due to the strained Si-I; 2) 150 and 470 cm^{-1}, characteristics of amorphous Si; 3) 387, 417 and 436 cm^{-1} due to Si-III, a body-centered cubic structure; 4) 505 cm^{-1} from the Si-IV, with a hexagonal diamond structure; 5) 167 and 353cm^{-1} of the Si-XII, a rhombohedral distortion of the Si-III and at 307 cm^{-1} due to disorder-activated second order transverse acoustic phonons at the boundary of the Brillouin zone. A similar rich spectrum with all these phases were obtained in cyclic nanoindentation tests and scratching experiments, and it is worth mentioning that some of these phases are unstable and are formed only with different time decompression rates according to Gogotsi et al. (1997). An interesting aspect about scratching experiments with different tool geometry was reported by Gogotsi et al. 2001; according to their work the amount of polymorphs in the groove produced by pyramidal tool was much less compared to the groove formed using spherical tool. It is worth mentioning that the tool geometry used in this work was single point diamond tool with nose radius and revealed a similar multiple phase.

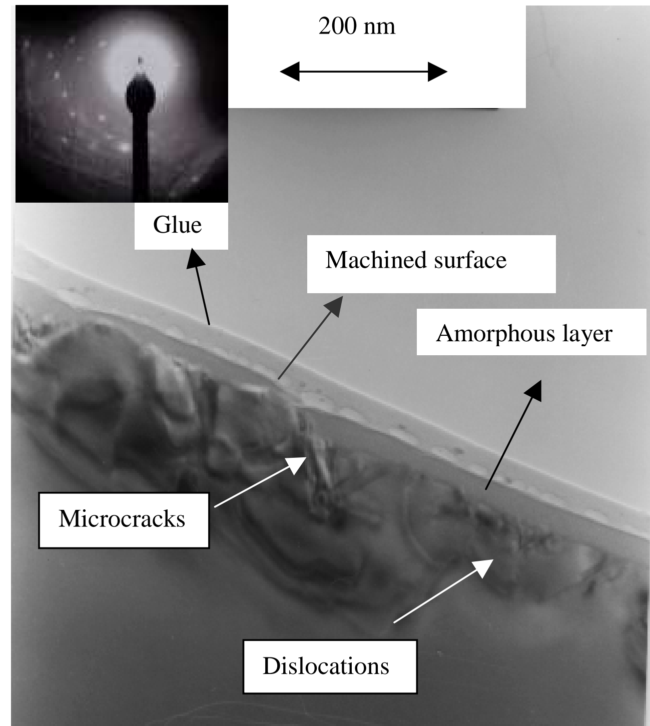

Figure 6. Bright field TEM images of the machined surface; a) cross-section view of the diamond turned surface(amorphous surface layer and subsurface microcrack) and detail of the EDP from the amorphous layer.

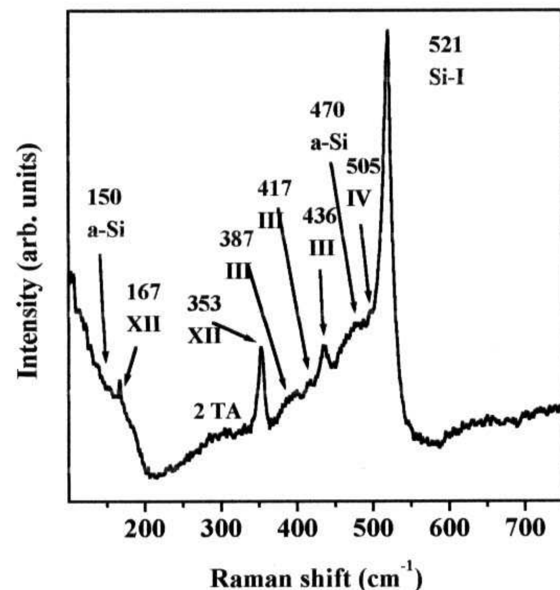

Figure 7. Raman spectrum of silicon debris on the diamond tool. Peak at 521.6 cm^{-1} due to cubic diamond structure of silicon single crystal (Si-I); at 519 due to the strained Si-I; at 470 and 150 cm^{-1}, of amorphous Si; at 436, 417 and 387 cm^{-1} due to Si-III; at 505 cm^{-1} from the Si-IV; at 353 and 167 cm^{-1} of the Si-XII, and at 307 cm^{-1} due to disorder-actived second order transverse acoustic phonons at the boundary of the Brillouin zone.

SEM image of small segments of ribbon-like continuous chips and of the machined surface are shown in Figure 8. Continuous chip formation can be considered as an evidence of the ductile response during machining. These chips are very thin and are likely to be formed at the vicinity of the tool tip centre and, a crack propagating

longitudinally along the chip surface is clearly observed in Figure 8. This portion of the chip is normally thin enough to have electron transparency. Energy dispersive spectroscopy (EDS) of the chips was carried out in the SEM apparatus and the results show that the quantity of oxygen is so small, that is hardly possible to say that the chip is oxidized. The results of the Energy dispersive spectroscopy (EDS) from the cut surface do not show any evidence of oxygen. This is done in order to discard the possibility of oxidation forming SiO_2.

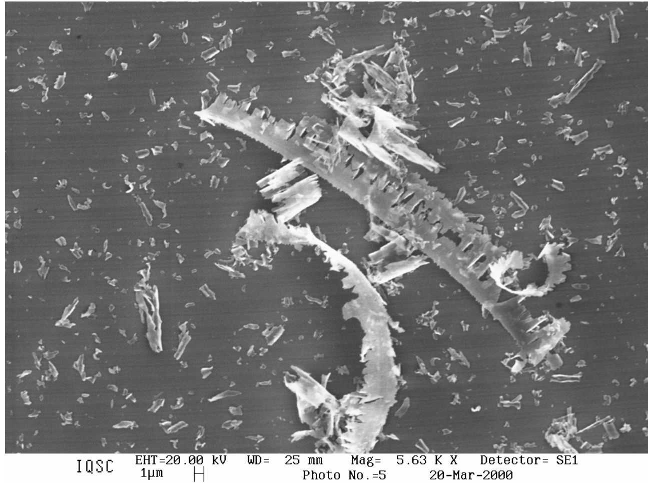

Figure 8. a) SEM photomicrograph of ribbon-like continuous chip found in the machined surface after cutting.

TEM examination of chips may provide important information on the mechanism of material removal. The morphology and structure of the chip were evaluated by Transmission Electron Microscopy (TEM). Figure 9 a displays a bright-field TEM image of a small part of a ribbon-like chip. Figure 9 b is an image of the selected area marked with a circle shown in Figure. 9 a. A lamellar pattern similar to that observed in ductile metals is observed on the free surface of the chip, resembling very small and thin plates. This is indicative that a shear deformation mechanism was involved during chip formation. The distance between lamellae, called shear front (Black, 1972) as well as the lamella size, are very small and difficult to be estimated. The shear front is a particular region of the chip where neither extruded material nor dislocations or crystallites are observed. Only sharp striations perpendicular to the cutting direction can be observed.

The electron diffraction pattern from this specific region of the chip (Fig 9 c) shows clearly a diffuse halo ring indicating amorphous phase. Since no signs of crystallite fragments are found in this portion of the chip, apparently this result does not corroborate with former works reporting the presence of crystalline phase immersed in an amorphous medium.

Bright-field TEM image of another chip (width ~5 μm) is shown in Figure 10. Two electron diffractions of the chip were carried out. The positions 1 and 2, marked in the photomicrographs, correspond to the electron diffraction pattern of the chip. The electron diffraction pattern from point 1 shows the diffuse halo ring indicating amorphous structure and the electron diffraction pattern from point 2 contains both halo rings and diffraction spots indicating the presence of a remnant crystalline matter.

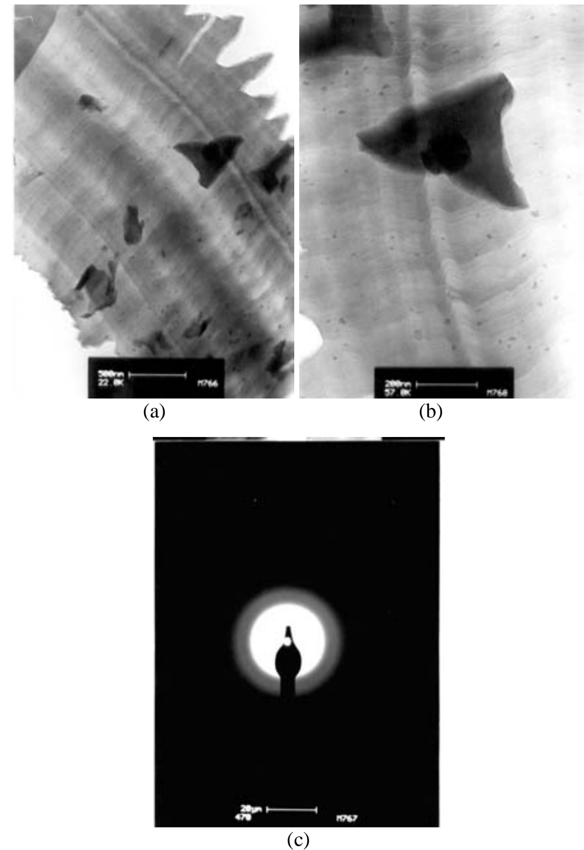

Figure 9. Ribbon-like continuous chip of (001) single crystal formed at submicrometre level depth of cut. (a) Bright-field TEM image of a part of a ductile chip; (b) detail view shown in (a) where very thin lamellar structure is indicated with arrows which is a sign of shear deformation mechanism during chip formation and; c) transmission electron diffraction pattern (TEDP) which indicates that the chip is amorphous; no sign of dislocations and crystallinity is found in the chip.

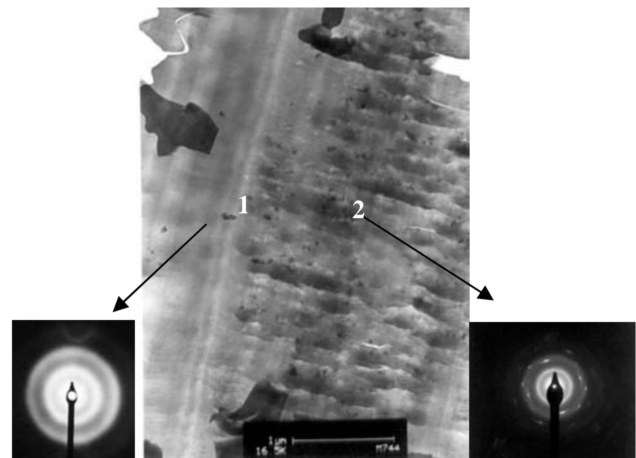

Figure 10. TEM image of chip, a) bright-field TEM image of a part of a ductile chip; electron diffraction pattern (EDP) from position 1 of the chip and electron diffraction pattern from position 2 of the chip. The chip presents amorphous phase and crystalline structure, simultaneously.

Figure 11 (a) shows a bright-field TEM image of a ribbon-like chip at low magnification showing a general view of the chip surface. This portion of the chip may be considered to belong to the body of a larger chip, which had been detached by means of a crack propagating longitudinally through the chip surface as in the chip

shown in Figure 8. Figure 11 b is an image of the area marked with a circle shown in Figure 11 a. This area can be considered the thinnest edge of the electron-transparent central area. The diffraction pattern from this area contains both halo rings indicative that the chip is amorphous and diffraction spots, suggesting the presence of remnant structured matter, as shown in Figure 11 c. The opposite portion of the same chip presents black blotches which did not show electronic transparency and thus could not be analysed with TEM.

Discussion

Based upon the exposed, it is possible to assert that the ductile material removal mechanism involved in single point diamond turning of silicon is resultant from transformation of different structural phases. It is likely that an extrusion-like process takes place below the brittle-to-ductile transition point in the shoulder, resultant from the compression forces acting in the "chip bulk" between the effective tool rake and the workpiece. The "sandwiched" crystalline phase does not transform completely within the amorphous medium, probably because of the reduction in stresses and is extruded from the edge/workpiece interface. This corroborates partially with the results reported by Komanduri et al. (2001) in which they could not assure whether this was a body centred tetragonal structure or an amorphous structure. Komanduri et al. (2001), based upon the distribution of interatomic distances and coordination numbers, suggest that the highly densified material in the chip, ahead of and underneath the tool is primarily the phase-transformed body centred structure. The near surface analyses detected the presence of a highly densified and not so well structured layer. This layer corroborates well with what it was referred to in the literature as a layer composed of silicon crystallites immersed in a silicon amorphous medium (Pizani et al., 1999). Since the size of this "sphere-like" pattern is found within the nanometer range, this result corroborates very well with those of Suzuki and Ohmura (1996) and Jasinevicius et al. (2000a) which assert that the sphere pattern can be judged to be a polycrystal formed by nanocrystals if the detected amorphization should be considered in an electron diffraction scale.

Since the transformation from β-tin phase to amorphous phase involves a volume increase, the material near the surface vicinity is not undergoing the same amount of compression and other silicon phases could be forming along the chip width. On the other hand, the material close to the tool radius centre is submitted to most of the compressive energy and is completely amorphous, as observed in Figure 9. The TEM analysis of the chips (Figure 9-11) confirms that they form within the transformed zone (very close to the tool tip) as indicated in Figure 2. This assertion corroborates well with three important results of other studies. First, the innermost and central regions of the marks in both indentation and scratching are totally amorphous. Second, shear deformation components lower the transition pressure necessary to attain the amorphous phase and, since lamellar morphology occurs in the chips, shear deformation components are likely to be present. Finally, very negative rake angles are expected to increase the hydrostatic stress within the transformed zone at the tool tip, as shown in Figure 12. Large hydrostatic stresses generate larger shear stresses which decreases the transition pressure value. Hydrostatic stresses also inhibit crack propagation (Castaing et al. 1981).

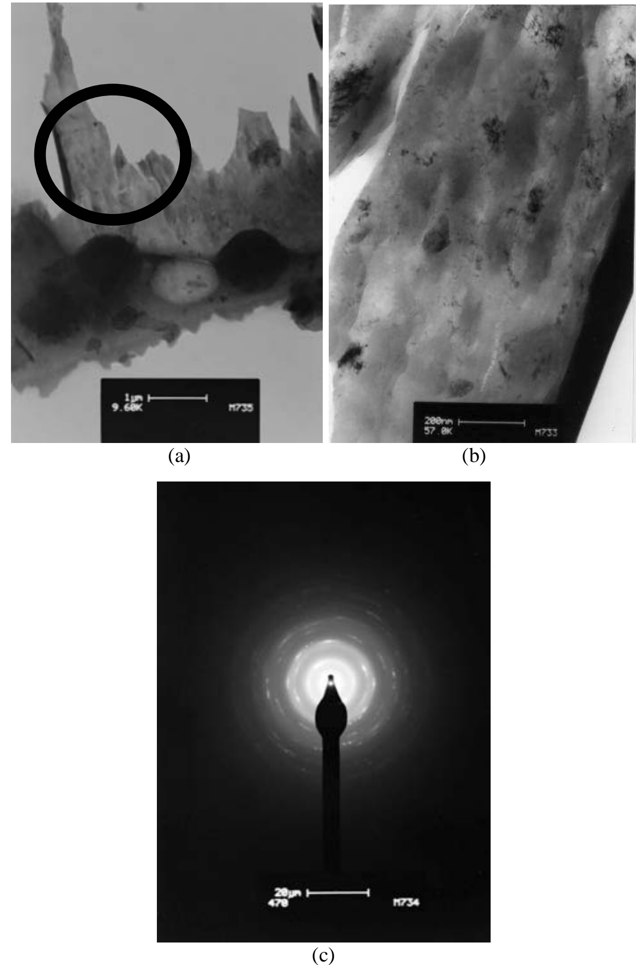

Figure 11. (a) Bright-field TEM image of a part of a ductile chip; (b) selected area, representing the thinner edge of the electron-transparent central area, marked with a circle shown in a), and c) electron diffraction pattern which indicates that the structure of chip is amorphous with some structured matter on it.

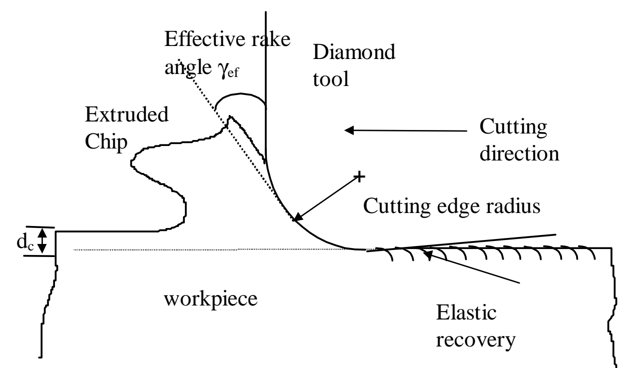

Figure 12. Schematic diagram showing the effective rake angle formed along the diamond tool face at cutting depths in the same range of the tool cutting edge radius.

In the machining process, due to the round form of the tool, there is a distribution of compression/decompression rates, leading to the simultaneous formation of several silicon phases. This process is illustrated schematically in Figure 13. Figure 13 a shows that up to the fracture damage depth y_c the chip area limited by the angle θ

increases with the depth of cut and, consequently, the stresses are reduced. (The real cross section of the chip, in Figure 13 b, is schematically represented with the calculated dimensions based on formulas found in Blake and Scattergood, 1990). According to Jasinevicius et al. (2000 b), the ductility of semiconductor crystals is inversely related to the transition pressure value. Since the chip contact area increases along the cutting edge, more difficult ductile removal of chips will be closer the uncut shoulder.

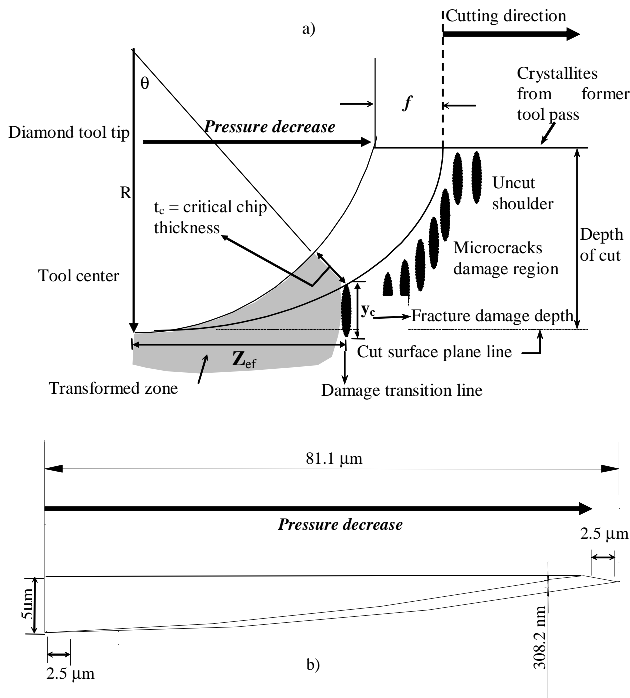

Figure 13. Schematic diagram of the cutting geometry for single point diamond turning with round nose tools. a) Transformed zone, b) chip cross section (undeformed); facing cutting direction.

The micro Raman spectrum presented in Figure 7 shows the presence of five different remnant structured matter in an amorphous medium in the silicon chips. Since these chips were analyzed at the tool rake surface and different phases were detected, it is reasonable to assert that they are resultant from decompressing multiple phase formation during machining of silicon, corroborating with scratching results presented by Gogotsi et al. (2001). According to the authors, the increase in the contact area between the tool and material generates insufficient pressure under the tool to drive the phase transformation and the plastic behaviour cannot be obtained.

Conclusions

TEM analyses of micromachined silicon surface and chips were performed to investigate the nature of the chip formation process. The main conclusions of this study are:

(1) Ductile material removal in silicon machining may involve two different and simultaneous processes: a shear lamellar formation and an extrusion-like process.

(2) Shear lamellar formation occurs at the tool centre vicinity because of the presence of totally amorphous lamellar structure, resembling that of soft metal chips. These lamellae are indicative of shear localization at high strain and high strain rates (Black, 1972; Morris et al., 1995).

(3) The extrusion-like process is related to chips presenting two different aspects: diffuse halo rings pattern which is indicative that the chip is amorphous and diffraction spots superposed on the halo rings revealing the presence of a remnant crystalline matter.

(4) The extrusion-like mechanism is attributed to an incomplete transformation of the crystalline phase "sandwiched" within the amorphous medium, because of the reduction in stresses, occurring within the edge/workpiece interface. Raman spectroscopy of the chips remaining on the rake surface of the tool shows five different phases of silicon.

(5) The subsurface damage induced by machining is deleterious but possible to be removed by a final chemical polishing process.

Acknowledgments

The authors would like to acknowledge the financial support of FAPESP, CNPq and CAPES (Brazil). The authors thank Professors José A. Varella and Mario Cilenci for providing the facilities for the TEM analyses at Departamento de Físico-Química, Instituto de Química - Universidade Estadual Paulista - Araraquara - SP – Brazil.

References

Black, J.T. 1972, Shear front-lamella structure in large strain plastic-deformation processes, *J. of Engg. for Ind., Trans. ASME, Series B*, Vol. 94**,** 307-315.

Blake, P.N., Scattergood, R.O., 1990, Ductile-regime machining of Ge and Si, *J. Am. Ceram. Soc*., Vol. 73, pp. 949-957.

Bradby, J.E., Williams, J.S., Wong-Leung, J., Swain, M.V., Munroe, P., J., 2001, Mechanical deformation in silicon by micro-indentation, Mater. Res., Vol.16, 1500-1507.

Callahan, D.L. Morris, J.C. 1992, of phase transformations in SI hardness indentations *J. Mater. Res*., Vol. 7**,** pp. 1614-1617.

Castaing, J, Veyssiere, P., Kubin, L.P., Rabier, J., 1981, The plastic deformation of silicon between 300°C and 600°C, *Phil. Mag. A*, Vol. 44, 1407.

Clarke, D.R., Kroll, M.C., Kirchner, Cook, R.F., Hockey, B.J., 1988, Amorphization and conductivity of Si and Ge during indentation, *Phys. Rev. Lett.*, Vol. 60, pp.2156-2159.

Gilman, J.J., 1992, Insulator-metal transitions at microindentations, *J. Mater. Res.,* Vol.**7,** 535-538.

Gilman, J.J. , 1993, Shear-Induced Metallization, *Phil. Mag. B*, Vol. 67, pp.207-214.

Gogotsi, Y. G., Kailer, A., Nickel, K. G., 1997, Phase transformations in materials studied by micro-Raman spectroscopy of indentations *Mat. Res. Innovat*., Vol. 1, pp.3-9 .

Gogotsi, Y, Baek, C.,Kirscht, F., 1999, Raman microspectroscopy study of processing-induced phase transformations and residual stress in silicon, *Semicond. Sci. and Technol*., Vol.14, pp.936-944.

Gogotsi, Y, Zhou, G., Ku, S. S., Cetinkunt; S., 2001,Raman microspectroscopy analysis of pressure-induced metallization in scratching of silicon, *Semicond. Sci. and Technol.* Vol. 16, pp.345-352.

Gridneva, I.V., Milman, Y.V., Trefilov, M., 1972, Phase transformation in diamond-structure crystals during hardness measurements, *Phys. Status Solidi A*, **14,** pp.177-182.

Gupta, M.C., Ruoff, A.L., 1980, Static Compression of Silicon in the [100] and in the [111] directions, *J. Appl. Phys*., Vol.51**,** pp.1072-1075.

Hu, J.Z., Markle, L.D., Menoni, C.S., Spain, I. L., 1986, Crystal data for high-pressure phases of silicon, *Phys. Rev. B*., Vol.34, pp**.**4679-4684.

JamiesoN, J.C., 1963, Science, Vol. 139, 762.

Jasineviciusa, R.G., Santos, F.J., PizanI, P.S., Duduch, J.G., Porto, A J.V., 2000**a**, Surface amorphization in diamond turning of silicon crystal investigated by transmission electron microscopy, *J. Non Crystal. Solids*, Vol.272, pp.174-178.

Jasineviciusb, R.G., Pizani, P.S., DuducH, J.G., 2000**b**, Brittle to ductile transition dependence upon the transition pressure value of semiconductors in micromachining, J. MATER. RES., VOL.15, PP.1688-1692.

Jasinevicius, R.G., Pizani, P.S., *unpublished results*, 2005.

Kailer, A, Gogotsi, Y.G., Nickel, K.G., 1997, *J. Appl. Phys.,* 81, 3057.

Komanduri, R., Chandrasekaran, N., Raff, L.M., 2001, Raman microspectroscopy of nanocrystalline and amorphous phases in hardness indentations, Phil. Mag. B, Vol. 81, pp.1989-1997.

Marshall, D.B., Evans, A.G., YakubI, K.B.T., Tien, J.W., Kino, G.S., 1983, The nature of machining damage in brittlle materials, *Proc. Royal Soc. London* A, Vol. 385 **,** pp.461-475.

Minomura, S., Drickamer, H.G., 1962, Pressure-induced phase transformations in Si, Ge, and some III-V compounds, *J. Phys. Chem. Solids*, Vol. 23, pp.451-456.

Minowa, K., Sumino, K., 1992, Stress-Induced amorphization of a silicon crystal by mechanical scratching, *Phys. Rev. Letters*, vol. 69**,** Vol.320-322.

Morris, J.C., Callaham, D.L., 1994, Origins of the ductile regime in low load scratching in Si, *J. Mater. Res*., Vol. 9 , 2907-2913.

Morris, J.C., Callaham, D.L.,Kulik, J., Patten, J. A. And Scattergood, R.O., 1995, Origins of the ductile regime in single point diamond turning of semiconductors, *J. Am. Ceram. Soc.*, Vol. 78, 2015-20120.

Pharr, G. M., Oliver, W.C., Harding, D.S., 1991, New evidence for pressure induced phase transformation owing indentation of silicon, *J. Mater. Res.*, Vol.6, pp. 1129-1030.

Pizani, P. S., Jasinevicius, R.G., Duduch, J.G. And Porto, A J.V., 1999, Ductile and Brittle damage in single point diamond turned silicon probed by Raman scattering, *J. of Mat. Sci. Lett*., Vol.18, 1185-1187.

Puttick, K.E., Rudman, M.R., Smith, K.J., Franks, A., Lindsey, K., 1989, Single-point diamond machining of glasses, *Proc. Roy. Soc. Lond. A*, Vol. 426, pp.19-30.

Puttick, K.E., Whitmore, L. C., Gee, A.E., Chao, C.L., 1994, Transmission electron microscopy of nanomachined of silicon crystals, *Phil. Mag. A*, Vol. 69, pp.91-103.

SHAW, M.C., Metal Cutting Principles, Clarendon Press, Oxford, 1984, Repreinted 1986, 593p.

Shibata, T., Ono, A. Kurihara, K., Makino, E., Ikeda, M., 1994, Cross-section transmission electron microscope observations of diamond turned single crystal Si surfaces, Appl. Phys. Lett., Vol.65, pp. 2553-2555.

Suzuki, T. Ohmura T.,1996, Ultramicroindentation of silicon at elevated temperatures, Philos. Mag. A, Vol.74, pp.10731084.

Wu, Y. Q., Shi, G.Y., Xu, Y.B. 1999, Cross-sectional observation on the indentation of [001] silicon, J. Mater. Res. Vol.78, pp. 2399-2401.

Zarudi, I., Zhang, L.C., 1999. Tribol. Int.., **32**, 701.

Zarudi, I., Zou, J., Zhang, L.C., 2003a. Microstructures of phases in indented silicon: A high resolution characterization, Appl. Phys. Lett., Vol. 82, pp.874-876

Zarudi, I., Zhang, L.C., Swain, M.V., 2003b., Behavior of monocrystalline silicon under cyclic microindentations with a spherical indenter, Appl. Phys. Lett., Vol.82, pp. 1027-1029.

Zarudi, I., Zhang, L.C., Swain, M.V., 2003c. Microstructure evolution in monocrystalline silicon in cyclic microindentations, J. Mater. Res., Vol.18, pp.758-761.

Zarudi, I., Zou, J., Mcbride, W., Zhang, L.C., 2004 Amorphous structures induced in monocrystalline silicon by mechanical loading, Appl. Phys. Lett., Vol.85, pp.932-934.